Automated, high precision measurement of critical dimensions using the atomic force microscope

Donald A. Chernoff[a] and David L. Burkhead

Advanced Surface Microscopy (ASM), Incorporated, Indianapolis, Indiana 46220-4955

We describe a computerized method to analyze the microstructure of optical disks. On digital versatile disks (DVDs), the smallest features are pits or bumps about 400 nm long, 320 nm wide, 120 nm high, with a track pitch of 740 nm. We measured the following parameters: track pitch, bump height, bump width and length (at various threshold levels), and four sidewall slope angles, in each case reporting the mean, standard deviation, and other statistics. In a single $10 \times 10 \, \mu$m image of a DVD stamper containing about 100 bumps, we tabulated about 1000 values. In a plot of bump width versus bump length, we found that the width at half height increased from 328 nm for the shortest bumps (440 nm long) to about 385 nm for bumps longer than 800 nm; this matches the increase seen for corresponding optical signals produced when a finished disk is played. Where a sidewall angle deviated from the norm, we were able to review the image data to identify the specific nature of the defect. This automated method yields statistically robust results, not only for mean values of structural parameters, but also for the standard deviations so that process windows can be determined. Thus, feature geometry will no longer be a hidden variable in the path between controlling production equipment and observing the good or bad electrical performance of a finished disk. © *1999 American Vacuum Society.* [S0734-2101(99)21404-2]

I. INTRODUCTION

Atomic force microscopes (AFMs) are used in many industries for research, engineering, and process control. Until now, AFM operators have usually made dimensional measurements by manually placing cursors on images or cross-sectional plots. Time constraints and operator fatigue limit the number of measurements. This in turn limits the extent of statistical analysis. We have developed an automated measurement process which overcomes these limitations and improves accuracy and precision.

High density optical disks such as digital versatile disks (DVDs) use nanometer technology: the smallest features are pits or bumps about 400 nm long, 320 nm wide, 120 nm high, with a track pitch of 740 nm. The size, shape, and placement of these marks must be controlled at the nm scale. Two particular specifications are

(1) The track pitch must have a mean value of $740+/-10$ nm and individual values must be in the range 710–770 nm. Given the fact that there are about 40 000 revolutions (tracks) on a given disk, this range suggests that tracks be placed with a standard deviation of 7 nm.

(2) The electrical pulse jitter during playback must have a standard deviation of less than 8% of the channel bit time. Converting time to length, we have a channel bit length of 133 nm and the jitter requirement is that leading and trailing pit edges be placed with a standard deviation of less than 11 nm.

There are many other electrical requirements which depend substantially on pit geometry, but the geometry itself is not specified. Although the manufacturer has considerable freedom in adjusting the pit geometry, it is wise to measure the pit geometry to maintain consistent quality.

The specifications mentioned above present a significant challenge for metrology. In order to make accurate pass–fail quality judgments, the ''gauge-maker's rule'' suggests that the measuring instrument be at least four times more precise than the product specification. Otherwise, money will be wasted when a good product is rejected and a bad product is accepted.[1] This implies that the track pitch measuring tool should have standard deviation <2 nm. Of course, the measurement procedure should be rapid, because it is necessary to measure many tracks (about 100) in order to get a useful estimate of the standard deviation. Let us first consider whether conventional scanning probe microscope (SPM) measurements can meet these requirements.

The old (or conventional) method of measuring track pitch using SPMs consists of capturing images and measuring point to point distances on cross-sectional profiles. The raw distance values are used directly, with the hidden assumption that the microscope calibration is perfect. When distances are measured in this manner, the pitch values are ''binned,'' with discrete values found at intervals corresponding to one pixel width in the original image. With a 512×512 pixel image, a scan size of 1 μm could be used to achieve a bin size of 2 nm. However, we would need to capture 100 images in order to make 100 observations of the track pitch. Similar difficulties apply to measurements of widths and slopes. For example, when measuring the feature width at half height, it is rarely possible to place the measuring cursors at exactly the desired height. In addition to imprecision (the 1 pixel limit), this method has the following defects: (a) the results are inaccurate due to scan nonlinearity

[a] Electronic mail: donc@asmicro.com

(see below); (b) the manual measurement process is tedious and slow.

In this article, we describe improvements in the AFM measurement process. The new, automated method provides a comprehensive approach to feature measurement, data analysis, calibration, and reporting. We show that pitch measurements in the *XY* plane are extremely precise (0.04 pixel, 1 std dev) and accurate to 1 nm (1 std dev).

After we describe our materials and methods, we present the following topics in Sec. III: (a) instrument characterization; (b) track pitch measurements; and (c) pit geometry measurements, including height, length, width, sidewall slope, and derived quantities such as length jitter and pulse length bias.

II. EXPERIMENTAL METHODS

A. Atomic force microscope

AFMs make three-dimensional images of solid surfaces. We used a Digital Instruments NanoScope® IIIA/dimension 3000 large sample AFM, operating it in air, using contact mode or TappingMode™. We calibrated the real-time scan control parameters using the factory-specified procedures, and obtained cosmetically acceptable images at all scan sizes. For the DVD work, we selected a scan size of either 10×10 or 15×15 μm. We captured height data only. We set the gains and scan rate to achieve accurate tracking of the hills and valleys. In order to improve the scan linearity, we set rounding=0.1, so that, when making a 10 μm image, the probe scanned 11 μm on the fast axis, while the AFM collected data for only the middle 10 μm of the scan. We used the same scan size, scan angle, and scan rate when imaging test and calibration specimens in a given run. Such consistency is needed to get the most accurate results.

B. Calibration and test specimens

We used three calibration reference specimens. When measuring track pitch only, we used a 288 nm pitch, one-dimensional holographic grating (MOXTEK) and we used either contact mode or tapping mode. When measuring the pit geometry, we used a 292 nm pitch, two-dimensional holographic grating, and scanned only in tapping mode. These two calibration gratings consisted of a silicon substrate with a patterned photoresist, overcoated with a tungsten thin film. We used a third holographic grating for instrument characterization. This was a 292 nm pitch, one-dimensional pattern of Ti lines on Si (MOXTEK). Because it was made by a different process, it provided an independent check of measurement precision. The holographic exposure process assures uniform feature spacing over the entire specimen area, with an expected accuracy of 0.1%. The fabrication and characterization of this material have been described in detail by Hansen et al.[2] Recently workers at the Korean standards laboratory have independently verified the mean pitch of similar MOXTEK specimens using optical diffraction measurements. For a one-dimensional grating with nominal period 288 nm, they found $287.593 +/- 0.005$ nm (the ex-
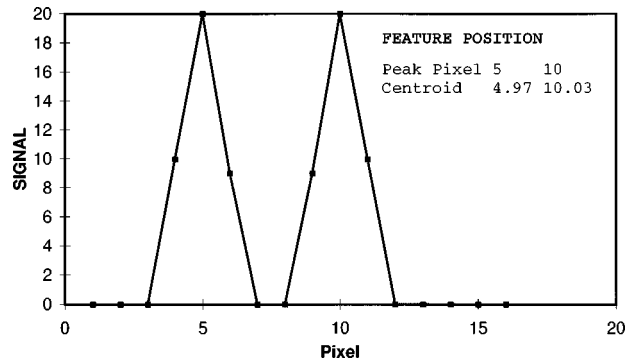

FIG. 1. Calculation of peak positions in a wave form. The peak pixel is always an integer, whereas the centroid is a real number. This allows subpixel precision.

panded uncertainty with coverage factor 2, i.e., a 95% confidence interval).[3] Although our calibration specimens are not yet officially traceable to the National institute of Standards and Technology (NIST), these results support our claim of 1 nm accuracy.

The test specimens were DVD stampers and uncoated replicas made with commercially available equipment.

C. Specimen orientation in the AFM

We typically selected a scan angle of 0° or 90°, which made the fast scan axis parallel to the *X* or *Y* physical axes of the scanner, respectively. We rotated the calibration specimen so that the ridge axis of the one-dimensional grating or one of the axes of the two-dimensional grating was parallel to the slow scan (*Y*) axis of the captured image within 2°. We translated the disk specimens as needed so that the tangential direction (along the length of the tracks) was also parallel to the slow scan direction.

D. Data analysis

The essential steps of our patented procedure[4] are as follows: (1) analyze the calibration image data to assess microscope accuracy, including the magnification error and nonlinearity. (2) Develop correction functions for the *X* and *Y* axes. These functions map the apparent position to the corrected position. (3) Analyze the test images to locate and measure the features of interest using the same procedures used for the calibration images. (4) Apply the correction functions to produce corrected measurement data for the test images.

In order to diagnose and correct calibration errors along the *X* and *Y* scan axes, it is necessary to compute very precise pitch values from the calibration images. We first calculated an average cross section parallel to each axis of each calibration image, using as much of the data as possible. We then used a proprietary feature finder in ASM's Calibrator Pro™ or DiscTrack Plus™ software.[4,5] This algorithm calculates feature locations with subpixel precision and can reveal subtle image distortions. The concept of subpixel measurement precision can be explained by a simple example. Figure 1 shows a wave form containing two peaks plotted as signal

level versus pixel number. When measuring the feature position using the location of the maximum value, the position is recorded as an integer. If we instead measure the feature position using the centroid or center of mass (here we use three points for each peak), the result is a real number, not an integer. This allows the possibility of subpixel precision. In our work, each feature location is typically the average of several thousand data points (pixels) in the original image. So the results are robust in the presence of noise spikes. Also, the center of mass calculation does not use an explicit model for the feature shape. This means that the pitch results are independent of the tip shape or variations in the surface characteristics from sample to sample. In principle, sampling errors could degrade resolution. For example, when the observed feature has a rectangular cross section, with 90° sidewalls, the edges are undersampled, and the position resolution (for any algorithm) is at best on the order of 1 pixel. In the present case, the average cross-sectional profile of the calibration grating was a smoothly varying function with 40° sidewalls; the absence of pathological oscillations was verified by higher resolution scans (AFM images of smaller fields of view; data not shown). In the calibration images actually analyzed, the edges were oversampled so that the 10%–90% rise was about 5 pixels wide and the features of interest in the test objects were even broader. So far we have only argued that subpixel resolution is possible. Whether subpixel resolution is actually achieved depends on the signal-to-noise ratio and other characteristics of the real data. We discuss an experimental test of our resolution below.

Although it is possible to use the distortion results displayed by Calibrator Pro to guide iterative adjustments of the AFM drive parameters and thereby improve real-time scan linearity,[6] we found it more convenient to capture images of ordinary linearity. We then used an additional algorithm, contained in DiscTrack Plus. This algorithm detects the nonlinearity of the SPM length scale using the calibration specimen as the reference, creates a linearized length scale, and applies that scale to the measurement results for the test specimen. We have found that this offline method gives results as good as the real-time method.[5]

We acknowledge some limitations of the measurements presented here. The height values were not corrected for Z axis measurement errors (1%–5%). The feature slope, width, and length have not been corrected for tip shape effects. The sidewall slopes of the test features of interest were in the range 25°–45°, which is much smaller than the shape limit (65°–80°) for the tips we used. Therefore, the slope measurements were not significantly affected by the tip shape. The bump width and length would be increased by the width of the tip apex, about 10 nm or so. In our discussion below we focus mainly on comparisons of relative width and length within and between test specimens (in order to see process trends) and on the precision of those parameters (in order to see process variation). When the same tip is used, such comparisons are valid even without calibrating and removing tip shape effects.
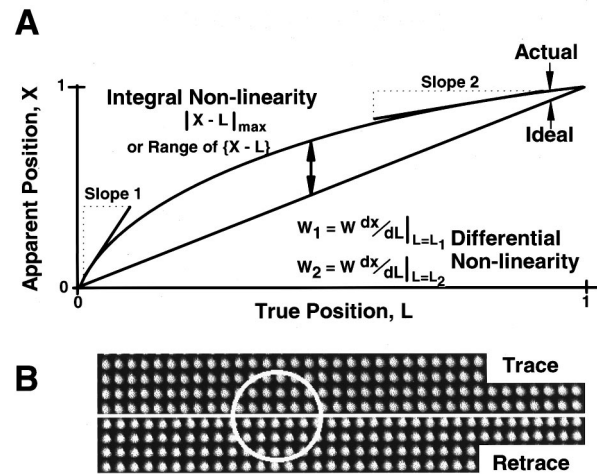

FIG. 2. Instrument linearity. (A) Integral nonlinearity affects measurements made between features that are far apart relative to the scan size and differential nonlinearity affects measurements of closely-spaced features. (B) Strips from AFM images of the 292 nm pitch calibration specimen. Note that the trace and retrace images line up at the edges but not in the middle. This is a qualitative indication of integral nonlinearity. 10 μm scan.

III. RESULTS AND DISCUSSION

A. Instrument characterization and measurement precision

All measurement tools, including microscopes, are subject to some distortion or nonlinearity. Figure 2(A) presents several concepts for analyzing nonlinearity. In an ideal microscope, the apparent position, X, of an object always equals its true position, L. For a real microscope, X differs from L and this deviation depends on the object's position in the field of view.

Integral nonlinearity measures the deviations of X from L, normalized to the overall scan length. This performance specification is relevant when measuring widely separated objects.

Differential nonlinearity measures variations in the slope of the apparent position curve. This specification is relevant when measuring nearby objects, such as pit widths or individual values of the track pitch. Variations in slope mean that an object of true width W would appear to have a larger width, W_1, at one location and a smaller width, W_2, at a different location. We assess differential nonlinearity by measuring the pitch of consecutive features on a finely spaced grating and we compute it using the following equation:

$$D = 100*[(P_O - P_M)/P_M], \tag{1}$$

where D = differential nonlinearity (%), P_O = observed pitch (individual value), and P_M = mean pitch (mean of all values).

Figure 2(B) gives a qualitative view of nonlinearity in a 10 μm scan of a calibration grating. If one views only the trace or retrace data, the eye cannot easily detect any nonlinearity; thus we say the scan is "cosmetically acceptable." However, by comparing two images side by side, the nonlinearity is plainly seen. If the scan had been linear, the feature
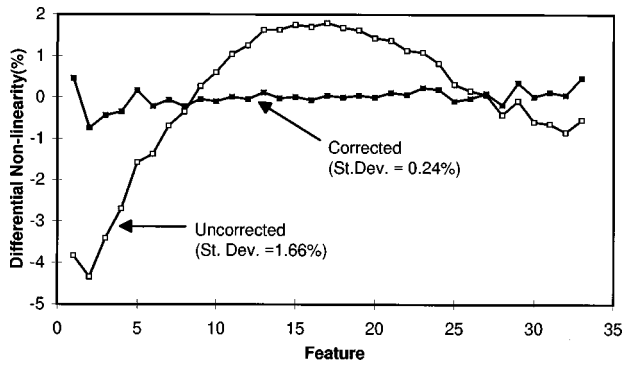
FIG. 3. Differential nonlinearity in a 10 μm AFM scan of one calibration grating, before and after correction of measurement data using results from a scan of a second calibration grating.
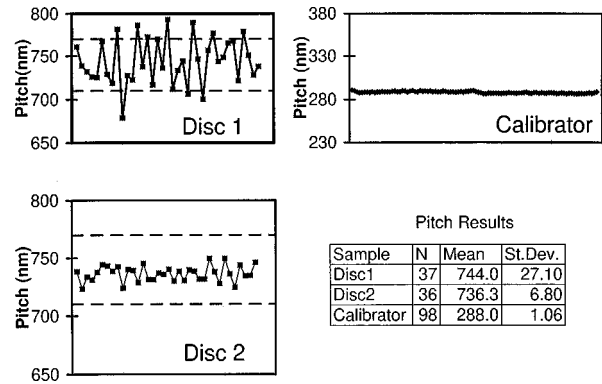

FIG. 4. Track pitch measured on two different DVDs. The graphs show individual pitch values, with the dashed lines indicating the specified upper and lower limits. The table shows summary statistics.

positions in images captured in the trace (left to right) and retrace (right to left) directions would match everywhere. The circle highlights an area where the integral nonlinearity is particularly noticeable.

To demonstrate a quantitative analysis of differential nonlinearity and to measure the precision of our correction method, we captured 10 μm images of two different one-dimensional calibration gratings. We measured the observed feature positions and pitch values for gratings A and B using the high precision measurement process described in Sec. II D. In Fig. 3, the curve labeled ''uncorrected''shows the observed differential nonlinearity for scan B: the standard deviation is 1.66%. Using the data from A, we computed the X axis correction function. We applied this function to the measurement data for B and computed corrected feature positions and pitch values. In Fig. 3, the curve labeled ''corrected'' shows that the differential nonlinearity was greatly reduced: the standard deviation was 0.24%, or 0.70 nm. Since 1 pixel in the original image was 19.5 nm, the measurement precision was 0.036 pixel. This uncertainty represents the overall precision of the pitch measurement process. This overall precision includes contributions from sources of error such as surface roughness and edge roughness of the calibration specimen, AFM noise, and sampling error. It is beyond the scope of this article to estimate the relative magnitude of each individual source of error.

B. DVD track pitch

We have discussed elsewhere why the track pitch is tightly specified and what equipment problems can cause the track pitch to be out of specification.[5] In order to measure the track pitch, we captured and analyzed 15 μm images of the one-dimensional calibration grating and of the test disks. Figure 4 shows typical results obtained from a set of such images. Although its mean pitch was acceptable, the first disk had several instances of pitch values outside the allowed range. In contrast, the second disk passed both specifications. The results for the calibration specimen are a self-consistency check. The standard deviation of 1.1 nm indicates the underlying precision of the track pitch measurement. This amounted to 0.038 pixel in the 15 μm image.

C. DVD pit geometry

The shape of the pits in the finished disk determines its electrical (playback) characteristics. Many engineers adjust production variables based on the outcome of electrical tests, treating pit geometry as a hidden variable. However, with an efficient way to measure geometry at various process stages (i.e., pits, bumps, and pits formed in the photoresist-coated glass master, nickel stamper, and molded replica, respectively) it will be possible to discover the links between production variables and pit shape and between pit shape and electrical characteristics. The features of interest include slope angles on all four sides, and the height, length, and width at various threshold levels. We focus here on just five parameters: left and rear slopes, height, and length and width at half height.[7] We report measurements of approximately 600 bumps on two different stampers, ''A'' and ''B''.

Table I shows the count, mean, and standard deviation for the height, width, and slopes of the two stampers. There were some similarities (mean height and sidewall angle) and some significant differences. The bump width was much larger for A (357 nm) than for B (302 nm). The standard deviations of the height and wall angle were about twice as large for A as for B. Now, consider that data encoding on DVDs uses 10 different feature lengths which are numbered according to their duration in ''channel bits'' (the fundamental clock period): T3, T4,..., T11, and T14.[8] Our data set is large enough that it is useful to classify the results according to bump length. Figure 5 is a graph of bump width as a function of bump length for B. Note that the width increases with length

TABLE I. Bump height, width, and sidewall slope for DVD stampers A and B.

	A		B	
	Mean	Std dev	Mean	Std dev
Height (nm)	96.95	6.19	95.28	2.50
Width (nm)	357.15	28.01	302.42	26.23
Left angle (deg)	38.48	5.80	37.17	3.27
Count	194		377	
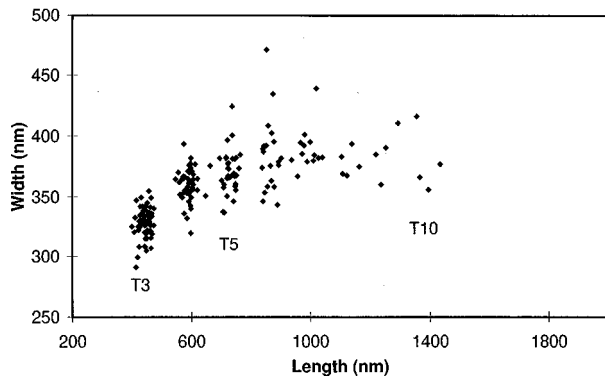
FIG. 5. Variation of width with length for bumps on DVD stamper A.

TABLE II. Edge jitter for DVD stampers A and B.

Parameter	A SD within group	B SD within group
Bump length (nm)	19.40	17.20
Land length (nm)	16.70	16.80
Edge jitter (nm)	12.80	12.00

for the T3–T5 bumps and is approximately constant thereafter. This corresponds to the well-known increase in amplitude of the high-frequency playback signal with length.[9] From this graph and from similar graphs of wall angle and height versus length, we identified ''outlier'' bumps. By reviewing the AFM images to inspect those specific bumps, we found that the larger standard deviations for stamper A were due to the presence of many bumps about 20–50 nm high. Such defects were not found on B, see Fig. 6. These defects would tend to increase noise and crosstalk during playback. The root cause can probably be found in the electroforming process which produced the stamper from the photoresist-coated glass master.

In order to investigate the contribution of an error in feature placement to electrical jitter, we need to compute geometric edge jitter. We cannot measure edge placement relative to any absolute location on the specimen, but we can infer edge jitter by analyzing the variability of the bump lengths and land lengths.[10] We labeled each observation with its T number and then did the one way analysis of variance (ANOVA-1) calculation. Table II shows the within group standard deviations for bump and land lengths. We then computed edge jitter as

edge jitter

$$= (\text{within group standard deviation of length})/\sqrt{2}.$$

The above equation is based on normal error propagation, where the variance of the overall length equals the sum of the variances of the positions of the front and rear edges. As shown in Table II, we found that the computed edge jitter approximately met the specification for both stampers.

In order to control the asymmetry of the high-frequency playback signal, DVDs can be mastered so that the mean lengths of the lands are larger than the lengths of the corresponding bumps or vice versa. Verhaart calls this a ''write strategy.''[11] We evaluated the write strategies for stampers A and B by linear regression of length versus T number. Table III shows the slopes and intercepts we found, as well as the goodness of fit parameters. The fits were excellent in
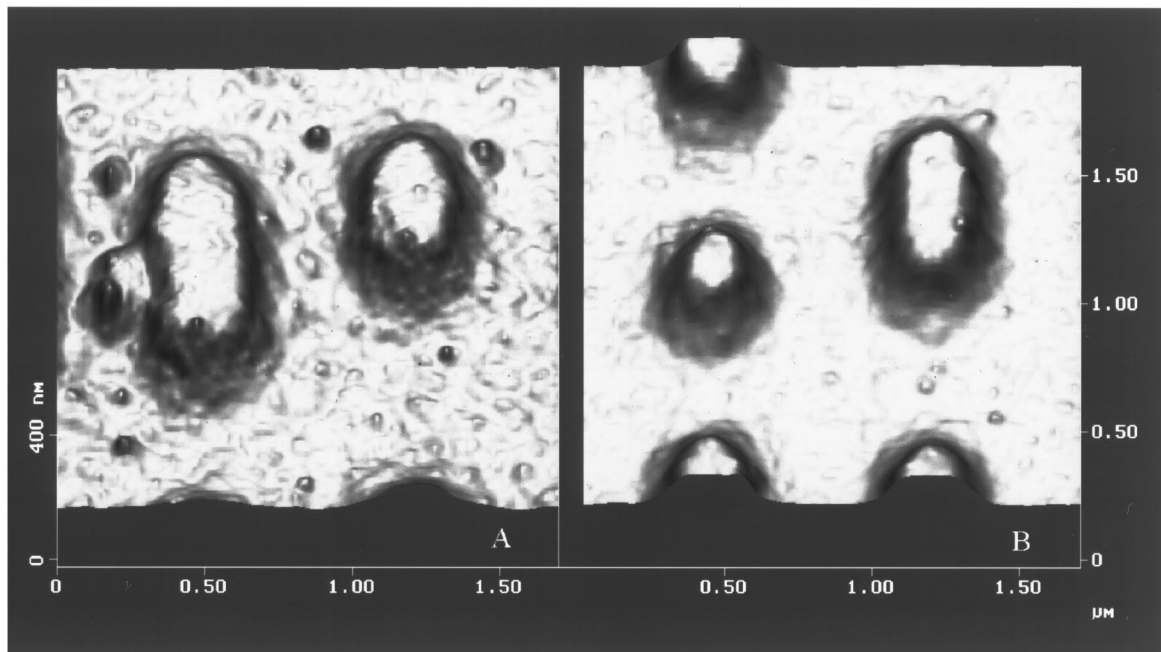

FIG. 6. Perspective view of AFM images showing defective bumps on stamper A and nicely formed bumps on stamper B. 1.7 μm scan rendered in slope mode.

TABLE III. Linear regression of length vs T number.

	Slope (nm)	Intercept (nm)
A, land	136.28	−44.37
B, land	137.22	30.76
A, bump	136.41	39.96
B, bump	138.57	−40.97

Goodness of fit parameters for all four fits:
SD, slopes=0.5–0.9 nm
SD, intercepts=2.5–4.1 nm
R squared >0.992
SD, regression=16.8–20.0 nm

all cases. The slopes were somewhat higher than the nominal channel bit length (133.3 nm). However, the intercept values for stamper A show that the bumps were biased longer than the nominal value and the lands were biased shorter. The opposite was true for B.

IV. CONCLUSIONS

We have developed a method for automated analysis of AFM images to measure critical dimensions. By incorporating a correction function derived from images of a calibration specimen, we were able to improve the precision and accuracy of a standard AFM by about 5–10×. We applied this method to the analysis of data marks on DVDs, a new type of high density optical disk. We were able to distinguish the quality of disks passing and failing the track pitch specification. We measured over 10 geometric parameters (height, width, length, wall angles, etc.) for more than 550 data bumps on two stampers. Statistical analysis and a cross reference between the data table and the AFM images allowed us to identify a single type of defect which was the root cause of the larger shape variations found for one stamper. We analyzed bump and land length variations and discussed their relationship to electrical jitter and signal asymmetry during playback. The impact of these results is that they provide direct feedback to the process engineer. Bump width is the consequence of laser focus in the laser beam recorder (LBR). Bias in bump versus land lengths is the consequence of programmed pulse duration in the LBR. With this method in hand, feature geometry and placement are no longer hidden variables in the overall production process. Supplementary material is at www.asmicro.com. The images are copyrighted by Advanced Surface Microscopy, Inc. and reproduced by permission.

[1] W. A. Levinson, Semicond. Int. **18**(10), 165 (Oct. 1995); **19**(2), 113 (Feb. 1996).

[2] D. Hansen, M. Lines, D. Chernoff, and J. Lohr, Proc. SPIE **3050**, 361 (1997); ASM sells these calibration specimens.

[3] O. Beom-h., W. Y. Song, B. C. Park, and Y. U. Ko, Proc. SPIE **3677**, (1999).

[4] D. A. Chernoff and J. D. Lohr, U.S. Patents Nos. 5,644,512 and 5,825,670.

[5] D. A. Chernoff, J. D. Lohr, D. Hansen, and M. Lines, Proc. SPIE **3050**, 243 (1997).

[6] D. A. Chernoff and D. L. Burkhead, Proc. SPIE **3677**, (1999).

[7] The width is the full width at half height measured across the bump. The length is the analogous quantity measured along the bump.

[8] The edges are transitions from bump to land and land to bump. During playback these are registered as logical 1. The absence of a transition is logical 0.

[9] K. C. Pohlmann, *The Compact Disc Handbook*, 2nd ed. (A–R Editions, Madison, WI, 1992), p. 87.

[10] The land length is the distance between the rear edge (at half height) of one bump and the front edge of the next bump.

[11] G. J. Verhaart, Replitech International June, 1997, Speaker Presentations, p. 383.